Polar Meteorol. Glaciol., **17**, 25–35, 2003

Effects of stopping the Mediterranean Outflow on the southern polar region

Wing-Le Chan and Tatsuo Motoi

Global Warming Research Program, Frontier Research System for Global Change, 3173-25 Showa-machi, Kanazawa-ku, Yokohama 236-0001

(Received April 7, 2003; Accepted July 22, 2003)

Abstract: The extent to which the southern polar region is sensitive to the stopping of the Mediterranean Outflow is investigated by using a global ocean-atmosphere coupled model. Two experimental runs, one (named the control run) with and the other (named the NMOW run) without exchanges of heat and salinity between the Mediterranean Sea and the Atlantic Ocean, are carried out in order to simulate the presence and absence of the outflow. Large responses in the sea surface temperature are found in both the northern North Atlantic and the Southern Ocean. For the NMOW run, the response in the Southern Ocean shows general decreases in sea surface temperature and salinity over a millenial timescale. Sea-ice thickness mostly increases, but is reduced in regions associated with increased sea surface temperature. The freshening of the Southern Ocean brings about a decrease in the density difference between the southern polar regions and the tropics. Consequently, the meridional overturning which transports Antarctic Bottom Water decreases.

key words: Southern Ocean, thermohaline circulation, Antarctic Bottom Water, North Atlantic Deep Water

1. Introduction

The Mediterranean Sea is of special interest due to its semi-isolation and high salinity. Despite its relatively small surface area and volume, it is thought to contribute significantly to global climate. Reid (1979) suggested that, in the absence of the Mediterranean Outflow Water (MOW), the high salinity and density of the deep Norwegian-Greenland Sea cannot be maintained. Consequently, not only would the very existence of North Atlantic Deep Water (NADW) be in question, but also the formation of Antarctic Bottom Water (AABW) may not occur. His analyses of salinity along an isopycnal surface suggest that the MOW flows northward as an eastern boundary undercurrent before rising near the Iceland-Scotland ridge and contributing directly to the salinity of the Norwegian-Greenland Sea. However, more recent studies (McCartney and Mauritzen, 2001; Bower *et al.,* 2002) support a shallow source hypothesis, whereby the cold dense waters in the Norwegian-Greenland Sea are derived from the North Atlantic Current. In this case, the MOW has a less direct influence on the inflow, but nonetheless remains a constituent of it.

Since the saline NADW eventually makes its way toward the Weddell Sea to form

AABW, before spreading into the Indian and Pacific Oceans (Reid and Lynn, 1971; Woodruff and Savin, 1989), it is of interest to investigate how changes in the MOW affect the southern polar region through deep water circulation. Indeed, during the Messinian salinity crisis, which occurred 5–6 million years ago, the cessation of the Mediterranean Outflow into the Atlantic, which resulted from complete isolation of the Mediterranean Sea, coincided with a temporary weakening in the formation of dense waters in the Norwegian-Greenland Sea (Blanc and Duplessy, 1982; Woodruff and Savin, 1989).

It has also been hypothesized that projected increases in the salinity of the water carried into the Atlantic Ocean by the Mediterranean Outflow could initiate a new glaciation, via changes in high latitude ocean-atmosphere circulation (Johnson, 1997). A recent study by Rahmstorf (1998) uses an ocean model coupled to a simple atmospheric energy balance model to investigate the sensitivity of the North Atlantic thermohaline circulation (THC) to the MOW and finds that such changes in its salt content are insufficient to bring about glaciation. Schnitker (1980) also discusses past evidence linking large changes in Antarctic glaciation during the Miocene to events occurring in the Mediterranean.

In the present study, an ocean general circulation model (GCM) similar to that above is fully coupled to an atmospheric GCM and used to focus on the Southern Ocean, to which little attention has been paid in previous studies of global deep and bottom water circulation. The extent to which the role of the MOW plays on the climate in the southern polar region will be investigated. It would be of interest to compare results with those of Manabe and Stouffer (1999, 2000) who studied global climate responses to discharge of freshwater into the North Atlantic Ocean. In their experiments, large temperature anomalies were found in the Southern Ocean.

2. The coupled model and experimental procedure

The global coupled ocean-atmosphere model used for the experiment is the same as that employed by Manabe and Stouffer (1999, 2000) at the Geophysical Fluid Dynamics Laboratory (GFDL) of NOAA. A GCM of the atmosphere and ocean are coupled through momentum, heat and water exchanges which occur once daily. Realistic geography is included and flux adjustments of heat and water are also considered.

The atmosphere GCM (Gordon and Stern, 1982) has 9 finite difference vertical levels and rhomboidal spectral truncation at wavenumber 15. It is integrated in time steps of 30 min. Calculated insolation is set to vary seasonally and cloud cover is dependent on relative humidity only. The land surface component uses the bucket model to compute the soil moisture budget; soil moisture in excess of 15 cm is treated as runoff.

The ocean GCM (Bryan and Lewis, 1979) consists of a finite difference mesh with a grid spacing of approximately 4.5° latitude by 3.75° longitude and 12 finite difference vertical levels. The time step is fixed at 2 hours. The horizontal and vertical viscosity coefficients are constant at all locations and taken to be $2.5 \times 10^9\,\mathrm{cm^2/s}$ and $50\,\mathrm{cm^2/s}$ respectively. The horizontal diffusivity is an exponential funtion of depth:

$$A_{HH}(z) = A_B + (A_S - A_B)\exp(-z/500), \quad (1)$$

where its value at the surface and near the sea bottom are given by the constants, $A_S = 5.0 \times 10^7\,cm^2/s$ and $A_B = 1.0 \times 10^7\,cm^2/s$, respectively and z is the depth in meters. The vertical diffusivity increases in the opposite sense with depth, assuming the form:

$$A_{HV}(z) = A_0 + (C_r/\pi)\tan^{-1}[0.0045 \times (z - 2500)], \quad (2)$$

where $A_0 = 0.8\,cm^2/s$ and $C_r = 1.05\,cm^2/s$. Sea-ice thickness is predicted from thermodynamic heat balance in a sea-ice model which includes ice advection by ocean currents.

The model was previously integrated for approximately 10000 years at GFDL. The final conditions, which show both atmospheric and oceanic components in equilibrium states, are used as initial conditions for the present experiments, performed on the NEC SX5 supercomputer.

Using the same initial conditions, the model is integrated for 5000 years in two separate runs: one in which the flow of the MOW through the Strait of Gibraltar is simulated (control run) and one in which it is cut off (NMOW run). For the former case, heat and salt transports between the two sides of the strait are computed in order to simulate exchange of water due to limited spatial resolution (Manabe and Stouffer, 1988). Heat transport is achieved by replacing the seawater temperature in the most westerly gridbox of the Mediterranean Sea and that in the nearest gridbox within the North Atlantic Ocean with their mean values. Similarly, the seawater salinities in the same grid boxes are replaced by their mean values to simulate salt transport. This is repeated at each time step and at the top 5 levels, which extend from the surface to a depth of about 600 m. The sinking and spreading of the MOW is thus represented in the control run.

The simulated MOW in the control run first appears in the Atlantic at depths of 750 m before sinking, although there appears a weak northward flow along the eastern boundary at similar depths. At depths of 1130 m, a westward flow, which joins the North Atlantic Current, is seen. A warm, saline tongue appears at these depths, with salinity and temperature values corresponding well to those of NODC (Levitus) World Ocean Atlas 1994 data. In the NMOW run, these features disappear completely as the salinity shows little variation across the same depth. The eastern boundary undercurrent is also no longer evident and a weakening in the North Atlantic Current is seen.

3. Results

Figure 1 shows the difference (NMOW run–control run) in sea surface temperature over the entire globe. Values are averaged over the entire 5000 year integration period, with negative values shaded and positive values white. Three areas where the NMOW run yields much lower values (shaded areas) can be seen. First, the northern North Atlantic, south of Greenland, corresponds roughly to the area where the MOW outcrops to the surface. The other two areas are in the Southern Ocean, the one situated in the Pacific sector being the more prominent, with a maximum difference of approximately $-1.5^\circ C$. The elongated region is confined mostly between latitudes $60^\circ S$ to $50^\circ S$ and stretches from longitudes $170^\circ W$ to $70^\circ W$. The other large decrease in SST within the

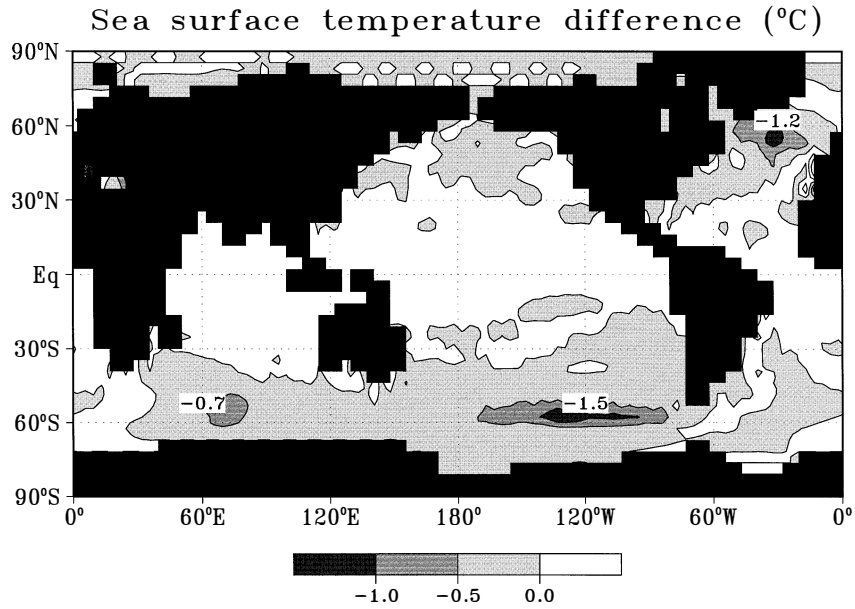

Fig. 1. Difference (NMOW run–control run) in sea surface temperature (depth 25 m), averaged over the 5000 years of integration. Negative values are shaded and contours are drawn in intervals of 0.5°C. The three labels refer to minimum values.

NMOW run is centered at 65°E, 55°S, south of the Indian Ocean, and covers a smaller and more even area. The maximum decrease in this case is about 0.7°C. The SST in the tropics and in much of the mid-latitudes increases only slightly, but extends over a larger area to maintain a heat balance.

Drawing attention to the time evolution of the SST differences (NMOW run–control run) within the Southern Ocean, mean values for each 1000 year period are depicted in Fig. 2 with accompanying changes in sea surface salinity (SSS) and sea-ice thickness (SIT). The spatial distribution of positive and negative SST differences varies little, except during the first 1000 year period when the value over much of the 90°E to 150°E sector of the Southern Ocean (*i.e.* south of Australia) is of the opposite sign. As expected, values of maximum anomalies are smaller than those of the remaining periods. The SSS shows a gradual decrease in value, which is counterbalanced by the increase in salinity within the Mediterranean. The areas of greatest SSS differences also show little change after the first 1000 year period. The largest decrease in SSS coincides with the maximal SST decrease in the Pacific Ocean sector. In general, positive (negative) SSS differences are found over areas where SST differences are positive (negative), apart from that in the high latitudes of the Pacific Ocean sector, across the Ross and Amundsen Seas where the SSS has increased. The SIT changes in accordance with the SST; the large SIT increase in the Ross Sea is associated with the SST decreases in the Pacific Ocean sector. Likewise, an equally large decrease in SIT is found at 0° longitude where the SST has increased. However, the SIT increase over the Indian Ocean sector is relatively small, despite a large SST decrease. Conversely, large SIT

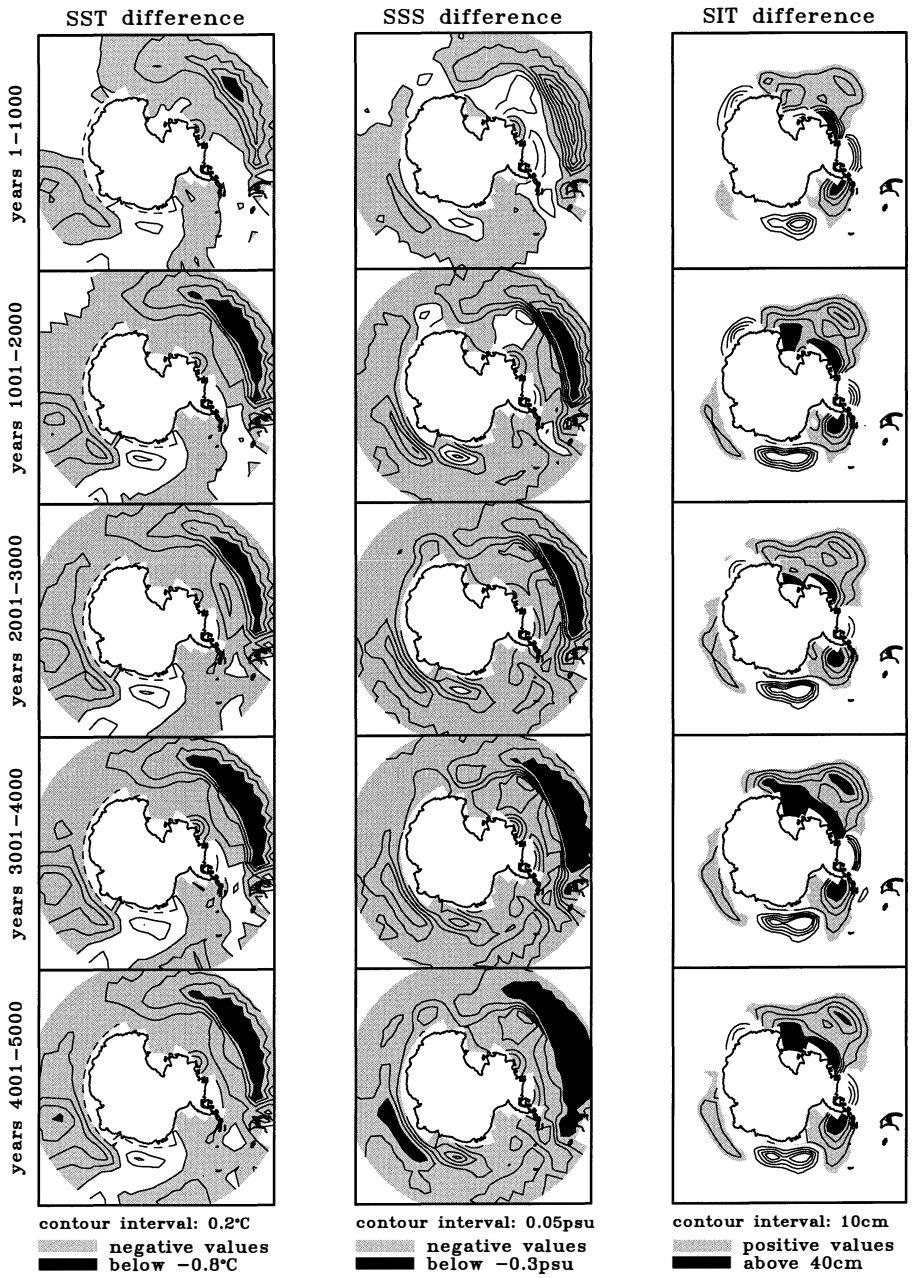

Fig. 2. Sea surface temperature (SST), sea surface salinity (SSS) and sea-ice thickness (SIT) differences (NMOW run–control run) within the Antarctic region, averaged over 1000 year periods. Positive SST and SSS and negative SIT differences are unshaded. Negative SST and SSS and positive SIT differences are shaded gray, except for extreme values which are shaded black. 0° longitude is in the downward direction of the page.

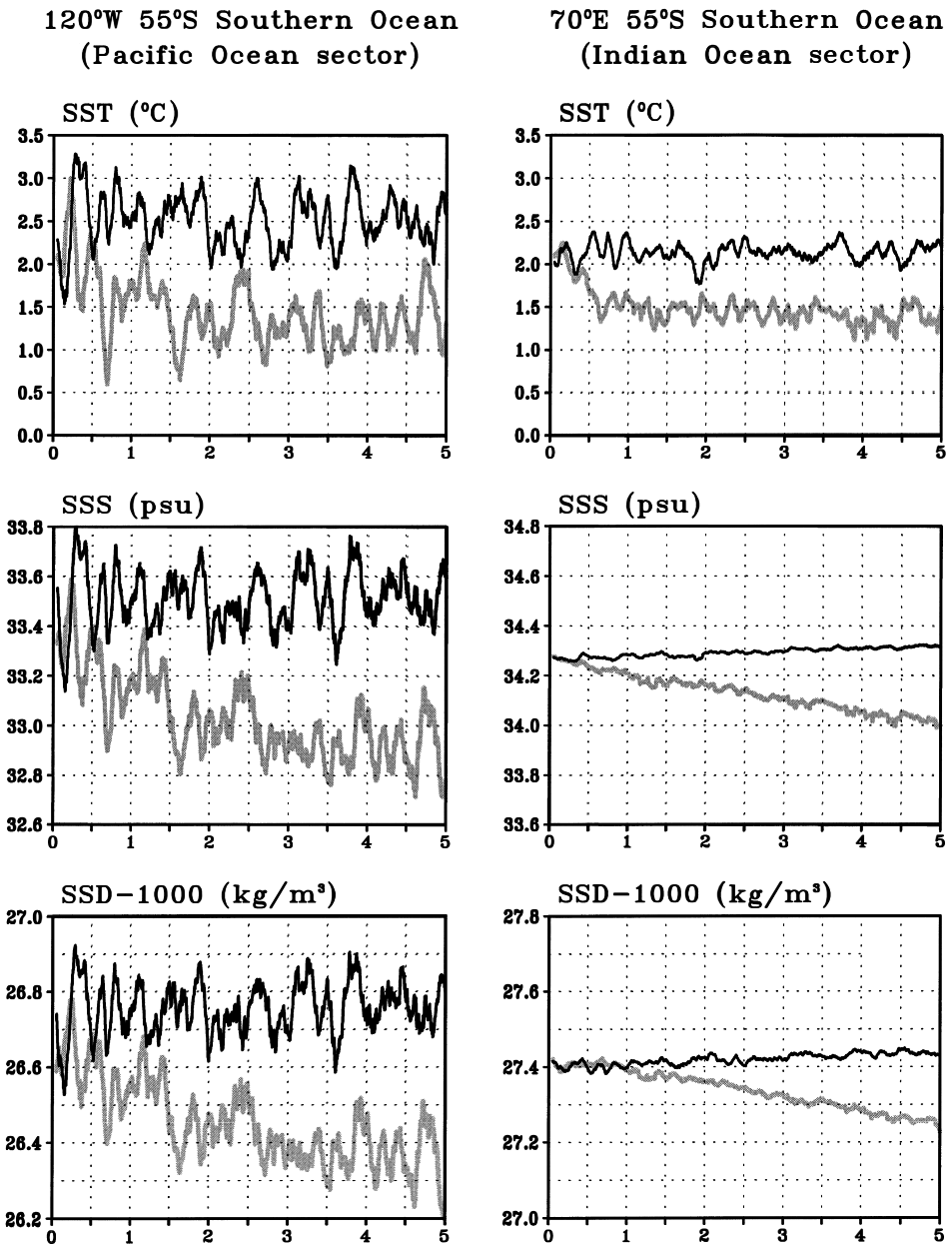

Fig. 3. Time series of sea surface temperature (SST), salinity (SSS) and density (SSD) at 2 locations in the Southern Ocean. The horizontal axes represent time in units of 1000 years. Black and gray lines refer to the control and NMOW runs respectively.

increases are found in the Weddell Sea where the SST decrease is small.

Time series of the SST, SSS and SSD (sea surface density) at the two locations of interest in the Southern Ocean are compared in Fig. 3. A 101 year running mean is applied to annual mean data in order to reveal centennial and longer timescale variability; this is also important in the Pacific Ocean sector as the large variability in the signals makes comparison difficult. Only after 200–300 years is there an evident reduction in the three variables in both locations, although the SSD in the Indian Ocean sector seems to show little change during the first 1000 years. The reduction in SST lasts for about 1000 years and those in SSS and SSD for slightly longer. Afterwards, the SST reaches a constant value. As the variability of the SST and SSS in the Pacific Ocean sector are both relatively large and of similar magnitude, it is clear that both are highly correlated and in phase with one another. The SSD follows the SSS closely due to the low

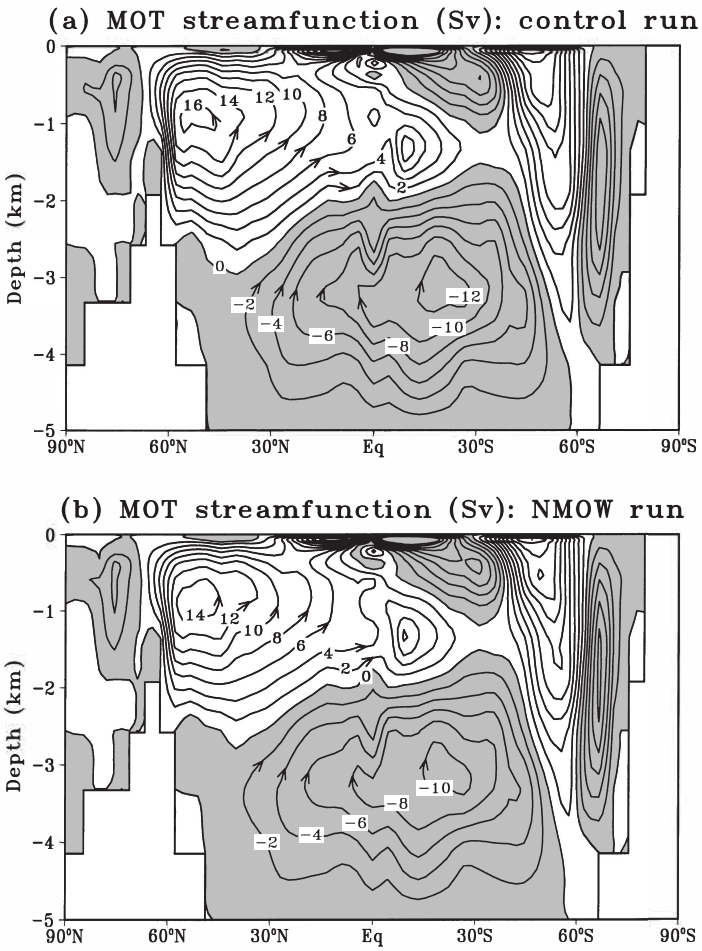

Fig. 4. Meridional overturning (MOT) streamfunction (Svedrups), averaged over 5000 years for the (a) control run and (b) NMOW run.

temperatures in the Southern Ocean.

The stream functions of the global meridional overturning (MOT) in the oceans for both runs are compared in Fig. 4, in which one can observe the structure of the North Atlantic Deep Water and the extent of the Antarctic Bottom Water (AABW) beneath. There are no large departures in the general patterns, although the intensities of both cells, defined as the maximum magnitude of the MOT, drop in value. The maximum differences between the two runs can be found at different locations from those of the maximum magnitudes. In the AABW, a maximum decrease of 3 Sv is located near the Equator, at a depth of 3.4 km, but this does not affect the maximum magnitude at latitude 20°S, depth 3 km, because of the difference in location.

Figure 5a shows the time series of the MOT intensity in the AABW cell for both

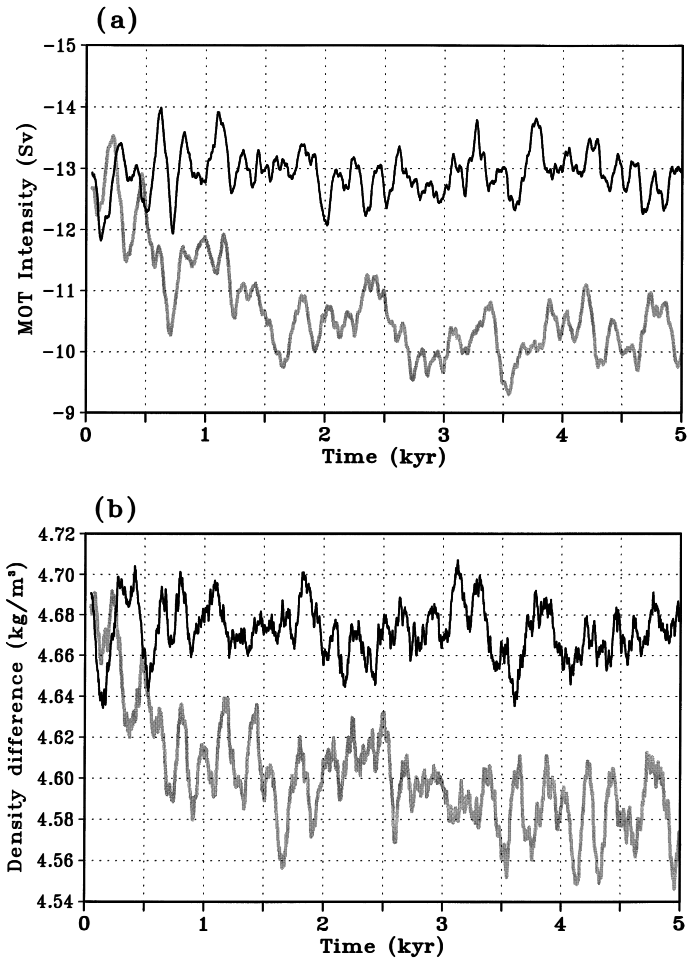

Fig. 5. Time series of the (a) meridional overturning (MOT) intensity of the Antarctic Bottom Water and (b) difference between the mean zonal sea surface density (SSD) at 55°S and at the Equator. Black and gray lines refer to the control and NMOW runs respectively.

runs and Fig. 5b the time series of the difference in the zonal mean SSD between latitude 55°S and the equatorial region. As in Fig. 4, a 101 year running mean is applied to annual mean data. Like SST and SSS, the MOT intensity exhibits a response time of about 200–300 years initially, after which it gradually starts to reduce before reaching an equilibrium state at approximately year 1500. Averaged over the last 3000 years of the integration, the MOT intensities are −12.9 Sv and −10.3 Sv for the control and NMOW runs respectively. This represents a 2.6 Sv reduction in the magnitude of the intensity. The time series of the difference in the zonal mean SSD displayed in Fig. 5b corresponds well to that of the MOT intensity. A temporarily increasing trend during years 1500–2500 can be observed in both time series.

4. Discussion

In general, the changes found in the Southern Ocean arise a few hundred years after stopping the Mediterranean Outflow at the start of the NMOW run and persist thereafter. The geographical distribution of the SST anomalies in the Southern Ocean and the time response are similar to those obtained by Manabe and Stouffer (1999, 2000), who conducted numerical experiments whereby a large amount of freshwater is discharged into the North Atlantic Ocean. They noted that, in one experiment whereby discharge occurs over the 50–70°N belt, cold anomalies in the Pacific Ocean sector continue to intensify for an additional 300 years or so after the discharge has ceased. However, their experiment shows SST anomalies in both the Pacific and Indian Ocean sectors of the Southern Ocean to be larger and of similar magnitude. Also, strong negative SST anomalies found by them in the South Atlantic Ocean sector are not found in the present study. Although the amount of freshwater discharge in their experiments does not equate to the loss of saline water in the NMOW run, they show that the location of the freshwater discharge is a major factor in the location and magnitude of the SST anomalies, which also explains the different results in their experiment and those of the present study.

Even though the model results show that the absence of the MOW does not greatly alter the pattern of the meridional THC, the reduction in the MOT intensity within the AABW is sufficient to bring about the changes which appear at the surface of the Southern Ocean. During the Messinian, when closure of the Mediterranean Sea is thought to have caused NADW formation to stop temporarily, the AABW, in addition to Circumpolar Deep Waters and Antarctic Intermediate Deep Waters, still formed (Blanc and Duplessy, 1982). However, results here show that the absence of the MOW has diminished the flow of the AABW more than that of the NADW.

While the experiments of Rahmstorf (1998) showed that relatively small changes in the salinity of the MOW are unlikely to lead to an increase in snowfall over Canada and the build up of ice sheets, as suggested by Johnson (1997), larger changes in the MOW may be sufficient to bring a larger response, not only in the northern polar region, but also in the southern. The present study shows both increases and decreases in sea-ice thickness in defined regions of the Southern Ocean, depending on changes in the SST. In particular, the thicker sea-ice in the Ross Sea produces an increased albedo which most likely accounts for the fact that surface air temperature there reduces by as much

as 6°C in the NMOW run (not shown). Schnitker (1980) argued that the NADW still reached the Antarctic during the Messinian, but was much less saline which led to reduced evaporation. This, in turn, led to a large reduction in the size of the Antarctic ice cap. Indeed, the snow depth over the Antarctic continent in the present study (not shown), apart from the region to the west of the Ross Sea, is predominantly lower, due to decreased snowfall because of decreased atmospheric moisture. However, decreases in snowfall are limited to the continent. The decrease seen here in warm NADW reaching the southern polar region may be too small to confirm the situation described by Schnitker (1980).

5. Conclusions

Numerical experiments in this study show that stopping the flow of MOW may induce strong surface signals in the Southern Ocean, resulting in general decreases in SST and SSS. These decreases are greatest in two locations. The more prominent one is found between latitudes 50°S and 60°S in the Pacific Ocean sector and has a maximum SST decrease of about 1.5°C. A smaller decrease of up to 0.7°C is found in a smaller region within a similar latitude range in the Indian Ocean sector. Small increases in SST are mostly confined to the South Atlantic sector.

The largest decreases in SSS are seen in the same two locations. As with SST, they are greatest in the Pacific Ocean sector. Although SIT increases in response to decreasing SST (and vice versa), the largest increases are seen in the Ross and Weddell Seas. There is a delay of about 200–300 years in the local response. SST and SSS then begin to decrease over a millenial timescale. The latter continues to decrease and dictates the SSD at low temperatures.

The MOT in the AABW shows little change in structure, except for a reduction from 12.9 Sv to 10.3 Sv in the intensity magnitude, defined as the maximum value of the MOW streamfunction. This represents a 20% drop. However, the greatest reduction in local volume transport occurs in the equatorial region of AABW. The changes in the MOT are brought about by the decreasing difference in density between the polar and equatorial regions, resulting from salinity anomalies.

Using analysis of Miocene benthic foraminiferal carbon and oxygen isotopic data, it has been suggested that closure of the Mediterranean Sea during the Messinian caused deep water formation in the northern hemisphere to weaken, or even cease, and NADW formation to greatly diminish (Blanc and Duplessy, 1982; Woodruff and Savin, 1989). The results here imply that the absence of the MOW alone brings about less drastic changes, but nonetheless exerts an influence on the climate of the southern polar region, by importing cooler, less saline water. A possible explanation for the difference is the changes in other major boundary conditions in the past, such as continental geography and topography. An important example is the closure of the central American isthmus which was not complete until 3 Ma ago, after the Miocene period (Mikolajewicz and Crowley, 1997). Before closure, NADW production may have already been weaker than at present due to exchange of saline water between the Atlantic and Pacific Oceans. Exclusion of the MOW under these circumstances could lead to yet weaker deep water formation.

Acknowledgments

The authors wish to thank Syukuro Manabe for his valuable advice and comments, Ron Stouffer for his assistance and for explaining the details of the model, Hyungmoh Yih for his contribution toward setting up the program and Kazuhiro Ban, who helped to improve its efficiency on the NEC SX5 supercomputer. Suggestions from two anonymous reviewers helped to improve this paper and are much appreciated. The authors accessed NODC (Levitus) World Ocean Atlas 1994 data which were provided by the NOAA-CIRES Climate Diagnostics Center, Boulder, Colorado, USA, from their website at http://www.cdc.noaa.gov/. This research was supported by Frontier Research System for Global Change.

References

Blanc, P.-L. and Duplessy, J.-C. (1982): The deep-water circulation during the Neogene and the impact of the Messinian salinity crisis. Deep Sea Res., **29**, 1391–1414.

Bower, A.S., Le Cann, B., Rossby, T., Zenk, W., Gould, J., Speer, K., Richardson, P.L., Prater, M.D. and Zhang, H.-M. (2002): Directly measured mid-depth circulation in the northeastern North Atlantic Ocean. Nature, **419**, 603–607.

Bryan, K. and Lewis, L.J. (1979): A water mass model of the world ocean. J. Geophys. Res., **84**, 2503–2517.

Gordon, C.T. and Stern, W. (1982): A description of the GFDL Global Spectral Model. Mon. Weather Rev., **110**, 625–644.

Johnson, R.G. (1997): Climate control requires a dam at the Strait of Gibraltar. EOS, **78**, 277, 280–281.

Manabe, S. and Stouffer, R.J. (1988): Two stable equilibria of a coupled ocean-atmosphere model. J. Climate, **1**, 841–866.

Manabe, S. and Stouffer, R.J. (1999): The rôle of thermohaline circulation in climate. Tellus, **51**, 92–109.

Manabe, S. and Stouffer, R.J. (2000): Study of abrupt climate change by a coupled ocean-atmosphere model. Quat. Sci. Rev., **19**, 285–299.

McCartney, M.S. and Mauritzen, C. (2001): On the origin of the warm inflow to the Nordic Seas. Prog. Oceanogr., **51**, 125–214.

Mikolajewicz, U. and Crowley, T.J. (1997): Response of a coupled ocean/energy balance model to restricted flow through the central American isthmus. Paleoceanography, **12**, 429–441.

Rahmstorf, S. (1998): Influence of Mediterranean Outflow on climate. EOS, **79**, 281–282.

Reid, J.L. (1979): On the contribution of the Mediterranean Sea outflow to the Norwegian–Greenland Sea. Deep-Sea Res., **26**, 1199–1223.

Reid, J.L. and Lynn, R.J. (1971): On the influence of the Norwegian–Greenland and Weddell seas upon the bottom waters of the Indian and Pacific oceans. Deep-Sea Res., **18**, 1063–1088.

Schnitker, D. (1980): North Atlantic oceanography as possible cause of Antarctic glaciation and eutrophication. Nature, **284**, 615–616.

Woodruff, F. and Savin, S.M. (1989): Miocene deepwater oceanography. Paleoceanography, **4**, 87–140.